Since January 2020 Elsevier has created a COVID-19 resource centre with free information in English and Mandarin on the novel coronavirus COVID-19. The COVID-19 resource centre is hosted on Elsevier Connect, the company's public news and information website.

Building and Environment 219 (2022) 109184

Contents lists available at ScienceDirect

Building and Environment

journal homepage: www.elsevier.com/locate/buildenv

Evaluating SARS-CoV-2 airborne quanta transmission and exposure risk in a mechanically ventilated multizone office building

Shujie Yan [a], Liangzhu (Leon) Wang [a], Michael J. Birnkrant [b], John Zhai [c,**], Shelly L. Miller [d,*]

[a] Dept. of Building, Civil & Environmental Engineering, Concordia University, 1455 de Maisonneuve Blvd. West, Montreal, Quebec, H3G1M8, Canada
[b] Carrier Corporation, 6304 Thompson Road, East Syracuse, NY, 13057, USA
[c] Department of Civil, Environmental and Architectural Engineering, University of Colorado, Boulder, USA
[d] Department of Mechanical Engineering, University of Colorado, Boulder, USA

ARTICLE INFO

Keywords:
Multizone
Whole-building
SARS-CoV-2
Infective risk
Airborne transmission
Wells-Riley

ABSTRACT

The world has faced tremendous challenges during the COVID-19 pandemic since 2020, and effective clean air strategies that mitigate infectious risks indoors have become more essential. In this study, a novel approach based on the Wells-Riley model applied to a multizone building was proposed to simulate exposure to infectious doses in terms of "*quanta*". This modeling approach quantifies the relative benefits of different risk mitigation strategies so that their effectiveness could be compared. A case study for the US Department of Energy large office prototype building was conducted to illustrate the approach. The infectious risk propagation from the infection source throughout the building was evaluated. Different mitigation strategies were implemented, including increasing outdoor air ventilation rates and adding air-cleaning devices such as Minimum Efficiency Reporting Value (MERV) filters and portable air cleaners (PACs) with HEPA filters in-room/in-duct germicidal ultraviolet (GUV) lights, layering with wearing masks. Results showed that to keep the risk of the infection propagating low the best strategy without universal masking was the operation of in-room GUV or a large industrial-sized PAC; whereas with masking all strategies were acceptable. This study contributes to a better understanding of the airborne transmission risks in multizone, mechanically ventilated buildings and how to reduce infection risk from a public health perspective of different mitigation strategies.

1. Introduction

The COVID-19 pandemic has caused more than 276.1 million people to be infected (including more than 5.3 million deaths) worldwide as of December 2021 [1]. Recently, its new variants are more contagious and caused more severe symptoms among younger people [2–4], driving another surge of cases worldwide. While vaccinations have been underway in many countries, there are still many regions and areas in the world that have made little progress in controlling the pandemic, such as India and Brazil [5,6]. It is likely that COVID-19 may linger longer than expected, turning into an "endemic" pathogen [7]. Therefore, we must be prepared for the possibility that COVID-19 is here to stay and also that other pandemics may occur in the future.

An important aspect of the COVID-19 pandemic is that the infection is transmitted by inhalation of airborne particles, or an aerosol, containing the SARS-CoV-2 virus. These particles are released by an infected person from their respiratory tract as they are breathing, talking, singing, *etc*. Although the size of the SARS-CoV-2 virus varies from 0.06 to 0.14 μm [8], the virus-containing aerosol consists of particles made of virus in a respiratory fluid, which is a complex mixture of various organic and inorganic constituents (water, salts, lipids, proteins, bacteria, other viruses) suspended in air; thus their size exceeds the diameter of the naked virus itself. So far, multiple sizes of airborne virus-laden particles for SARS-CoV-2 have been detected, ranging from 0.25 μm to 5 μm [9–13], which enables them to be easily transported over long distances.

Close contact with infected individuals, poor ventilation, no air cleaning, and prolonged exposure time indoors are the main reasons for elevated risk of transmission and infection in buildings [14]. Building ventilation is essential to dilute and remove aerosol, especially in highly occupied spaces. Air cleaning can both inactivate and remove aerosols through strategies such as germicidal ultraviolet light and physical filtration [15]. Short-range and long-range transmissions occur indoors,

* Corresponding author.
** Corresponding author.
E-mail address: shelly.miller@colorado.edu (S.L. Miller).

https://doi.org/10.1016/j.buildenv.2022.109184
Received 22 February 2022; Received in revised form 19 April 2022; Accepted 9 May 2022
Available online 13 May 2022

Nomenclature

A_L	Leakage area (m^2)
B	Breathing rate (m^3/s)
C	Contaminants concentration in the air (quanta/m^3)
C_D	Flow discharge coefficient
C_i	Contaminant concentration in the infectious zone (quanta/m^3)
C_j	Contaminant concentration in neighbor zones (quanta/m^3)
C_s	Contaminant concentration of the supply air (quanta/m^3)
C_{rec}	Contaminant concentration of the recirculation air (quanta/m^3)
C_{oa}	Contaminant concentration of the outdoor air (quanta/m^3)
F_m	The percentage of mask wearing occupants
G	Generation rate of quanta from the infector (quanta/m^3)
M	Removal efficiency of masks (%)
M_{inh}	Inhale removal efficiency of masks (%)
M_{exh}	Exhale efficiency of masks (%)
n_q	Number of inhaled quanta
N_c	Number of infection cases
N_s	Number of susceptible individuals
Q	Volumetric flow rate (m^3/s)
Q_r	Volumetric flow rate of the return air (m^3/s)
Q_{lx}	Volumetric flow rate of the local exhaust air (m^3/s)
Q_{ac}	Volumetric flow rate of the air cleaner (m^3/s)
Q_{UVr}	Equivalent volumetric flow rate of in-room GUV devices for pathogen inactivation (m^3/s)
Q_{dep}	Equivalent volumetric flow rate of aerosol deposition (m^3/s)
Q_{dec}	Equivalent volumetric flow rate of viral aerosol decay/inactivation (m^3/s)
Q_{exf}	Exfiltration flow rate to neighbor zones (m^3/s)
$Q_{inf,j}$	Infiltration from zone j (m^3/s)
$Q_{exf,j}$	Exfiltration from zone j (m^3/s)
t	Time (s)
V	Volume (m^3)
η_{ac}	Filter efficiency of the air cleaner (%)
η_{MERV}	Filter efficiency of MERV filters (%)
η_{UVd}	Inactivation efficiency of in-duct GUV devices (%)
Δt	Exposure time (h)
ΔP_r	Reference pressure difference (Pa)
$\Delta P_{j,i}$	Pressure difference between zone j and zone i (Pa)

with the difference being that at short range, the airborne particle concentration is much higher. Long-range transmission occurs when the aerosol travels long distances and accumulates indoors (typically beyond 1–2 m) [16]. Both the Federation of European Heating, Ventilation and Air Conditioning Association (REHVA) [17] and the American Society of Heating, Refrigerating, and Air Conditioning Engineers (ASHRAE) [18] recognized that building ventilation plays an important role to limit the risk of transmission [19,20]. In the guidance of re-opening buildings, ASHRAE [21] (as of September 2021) suggests at least the minimum amounts of outdoor air for ventilation needs to be adopted, combined with recirculation filters MERV13 or higher. Or alternatively, the combined effect of outdoor air, filtration and air-cleaning devices can achieve this level (minimum ventilation + MERV13). In addition, flushing rooms before and after occupancy, installing in-room germicidal ultraviolet lights (GUV), and equipping by-passing heat recovery sections were also recommended [18]. In comparison, REHVA as of April 2021 recommends applying the principle *As Low as Reasonably Achievable* pollutant concentration to set the required ventilation rate and setting the demand-control ventilation setpoint to 550 ppm CO_2 (absolute value) as an indicator of good ventilation. They also recommended using as much outdoor air as reasonably possible and open windows more than normal if thermal discomfort is not a concern; the recirculation dampers are required to be HEPA filters or at least have a particulate matter efficiency of 80% for an optical diameter between 0.3 μm and 1.0 μm based on ISO 16890 [22]) (termed ePM1) as compared to the equivalent level of 50% of a MERV 13; germicidal UV lights may be used in return air ducts or in rooms if they can be correctly sized, installed, and maintained; and by-passing the heat recovery section and avoiding potential leaks. Many Canadian guidelines follow ASHRAE. For example, the Insititut national de santé publique Quebéc (INSPQ) recommends as of Jan 2022 applying adequate ventilation to occupied buildings, especially if there are infected individuals inside the building [23].

In response to the COVID-19 pandemic, the ASHRAE Epidemic Task Force has provided some guidelines for commercial buildings and schools [24,25]. It was pointed out that a holistic framework would be needed for reducing exposure to SARS-CoV-2. In addition, general guidelines and suggestions for several specific spaces were provided, including lobbies, elevators and conference rooms *etc*. However, for a specific type of indoor space, their mechanical systems, configurations and operations are variable and need to be assessed on a case-by-case basis. To evaluate transmission risk and develop building/space specific mitigation strategies, many studies have been conducted. Jimenez et al. [26] developed a publicly available spreadsheet known as the "COVID-19 Aerosol Transmission Estimator" (COVID-19 Estimator hereafter). The tool provides information on key input parameters based on recent COVID-19 studies and makes it possible to evaluate infection risks and mitigation strategies and has been detailed in a paper by Peng et al. [27]. Existing tools, e.g., Jimenez et al.'s estimator, have been used to evaluate mitigation measures that reduce airborne transmission risk in specific cases, e.g., an indoor choir practice, classrooms, subways, supermarkets, and sports stadiums. Dai and Zhao [28] calculated the required ventilation rate to lower infection risk under 1% for different exposure times using the Wells-Riley model [29]. They modeled typical scenarios and concluded that the minimum required ventilation rate can be reduced by a quarter by wearing a mask, which can be achieved by the normal ventilation mode in most buildings. Lelieveld et al. [30] estimated the infection risk in several indoor environments, concluding that wearing a mask and actively ventilating rooms reduces risk by 5–10 times and is comparable to high-efficiency particulate filtering.

A study by Peng et al. [27] showed that multiple layers of protection, such as occupancy and exposure-time reduction, mask wearing, increased ventilation rates, and air cleaning through HEPA filtration and GUV disinfection, are important to reduce the COVID-19 infection risk to low levels. This is particularly true during the current situation of new variants such as Omicron. Zhang [31] estimated that by integrating different mitigation strategies for schools and offices, including source control, ventilation, and air cleaning strategies, infection risk could be reduced by a factor of 9–500. Sun and Zhai [32] modified the Wells-Riley model by introducing two indices for social distancing and ventilation effectiveness and showed that half occupancy density could reduce the infection risk by 20–40% in the first 30 min of an event. In a later study conducted by Ali et al., an archetype library of 29 building types was developed based on standards and references, and data were made available through an interactive website [33] using Jimenez's approach [27]. The urban archetype buildings allow decision-makers and managers to compare various mitigation strategies and generalize conclusions when urban-scale data are not readily available. As a demonstration, the impact of six mitigation measures on infection risks in various building types were evaluated. Additionally, Jialei et al. [34]

evaluated the effectiveness of control strategies in mitigating the infection risk in different scenarios and building types, including increased outdoor airflow rates, high-efficiency filters, advanced air distribution strategies, standalone air cleaning technologies, personal ventilation, and face masks.

Many of these works have focused on evaluating risks in single zones only. Empirical evidence has been reported for aerosol zonal transmission in an Eastern Canadian hospital [35]. Taewon et al. [36] have also suggested the possibility of SARS-CoV-2 transmission between different floors of an apartment building. In their epidemiology investigation, five of nineteen reported cases claimed no direct contact with other residents in the building. In Spain, it was reported that bathrooms of older buildings with communal ducts may have allowed aerosol exchanges [37].

One multizone simulation study by Emmerich et al. [38] applied the simulation software, CONTAM, for two infectious agents, a tuberculosis-like particle with a diameter of 0.64 μm and a burst emission, and a squamous cell particle with a diameter of 10 μm released at a constant generation rate. The study showed the importance of building leakage and the impacts of an actual building system operation. Although their study targeted healthcare facilities, it illustrated the importance of addressing the interactions of weather conditions, mechanical system operations, pressure differentials, and inter-zonal leakages in terms of airborne virus transmission. These interactions cannot be addressed systematically without a multizone building environment modeling approach. Another multizone contaminant transport simulation was also performed in a hospital building to evaluate existing air-cleaning strategies; the importance of building leakages was highlighted [39]. Prateek et al. simulated the indoor dispersion of airborne SARS-CoV-2 aerosols in a medium office CONTAM model and found that the unventilated stairwells are vulnerable to airborne viruses [40]. Shen et al. [34] pointed out that their study represented the most typical configurations for a building/space type, whereas a specific building could be more complicated, and the transmission risk depends on specific configurations [31]. On the other hand, a building ventilation renovation is often performed at the whole-system scale, so different rooms/buildings with rooms and indoor and outdoor interactions are essential. Indeed, a study on multizone buildings for specific building types is important with the reopening of public buildings. Building-wide protection instead of room-level protection will need to be evaluated with realistic weather conditions, air leakages, and occupancies. This will help identify loopholes in the renovation strategies, improve mitigation effectiveness and efficiencies, and develop building- and climate-specific, schedule-specified solutions to meet the variable, post-covid era needs. A few recent multizone simulation studies based on Modelica [41,42] show the importance of pressure controls and leakages in a hospital building [41] and HVAC filtrations on energy costs in an office building [42]. In addition, López-García et al. linked a zonal ventilation model with a multicompartment SIS Markovian model for evaluating the infection of patients within a hospital ward [43]. However, the inter-zonal airflows model have not been studied in depth in a detailed airflow network by the previous studies [39] and the airborne zonal infection transmission in commercial buildings were rarely investigated.

Conducting multizone analysis of airborne disease transmission in buildings with a more physically-realistic setting has many benefits from an occupant's health, safety, and productivity perspective and for energy-efficient operation during regular or emergent operations such as a pandemic. Many countries and governments have recently realized the importance of building ventilation and released new initiatives encouraging retrofits of existing buildings for reopening and future epidemics and pandemics. However, investing governmental funds to achieve healthy, safe, and energy-efficient goals needs to be addressed, considering the complexities of buildings and their multi-factorial interactions. Furthermore, the general public guidelines provided in the early and current stages of the pandemic may not be adequate. Thus a physically-realistic analysis tailored for different building types and climates should be conducted. This paper adopts a multizone simulation tool, CONTAM, to model SARS-CoV-2 transmissions in a US DOE prototype building, which represents a generic yet realistic building of a specific category in the US, and further estimates exposure risks based on the Wells-Riley model by considering the dynamic interactions of many influential parameters, including weather, occupancy, system operation, and temperature variation. The goal is to evaluate the multizone risks of airborne transmission of viruses and compare mitigation strategies in the context of a whole building compared to a single space. The final simulation input project and output files of the US DOE prototype buildings are also shared with this submission for future readers to apply the same approach to other building types. The files can be downloaded from this link: https://github.com/CUBELeonwang/CONTAM-Multizone-DOE.

2. Methodology

2.1. Multizone contaminant transport model

This study develops and demonstrates a new modeling approach for SARS-CoV-2 transmission risk in multizone mechanically ventilated spaces based on CONTAM. The US National Institute of Standard and Technology's multizone airflow and indoor air quality model CONTAM [44] implements simulations using DOE prototype commercial building models based on EnergyPlus [45]. CONTAM can analyze the complex and dynamic interactions of ambient conditions, building system operations, and occupancy behaviors in a more physically-realistic setting. Although EnergyPlus has an internal "airflow network" model, which is based on an earlier version of AIRNET [46] and COMIS [47], it has many limitations and is not designed for multizone analysis of pollutant transmission but instead for estimation of ventilation-related energy loads. It is also not included in the well-known EnergyPlus models of prototype buildings to reduce simulation costs.

Using this approach, we evaluate the potential for SARS-CoV-2 airborne aerosol transmission and exposure risk in mechanically ventilated multizone spaces and specifically address:

- the risks of room-room and floor-floor spreading,
- building mechanical system operations, including schedules and flow rates,
- leakages, pressure differentials, and room temperature schedules, and
- occupancy schedules.

If room-room spreading is significant, we also use the model to identify potentially vulnerable neighbor zones other than the source zone. If room-room spreading is relatively low, we investigate the impacts of single-zone mitigation strategies performed in the context of actual building operation in a multizone environment. Compared to existing SARS-CoV-2 models and tools, such as the single-zone model, FaTIMA [48], and multizone models based on Modelica [41,42], the proposed approach models whole-building multizone exposure risks [29]. Some recent multizone studies include risk models, such as Pease et al. [39], which, however, did not solve the airflow network. In comparison, the proposed approach covers both detailed multizone airflow and risk estimations for the DOE prototype buildings.

2.2. Airborne transmission under various mitigation approaches

In the context of the multizone simulation of airborne transmission, the concentration of virus-containing aerosol is estimated based on a mass conservation equation, Eq. (1) [49]. The time-change rate of the concentration in zone i $C_i(t)$ with volume V is a function of the generation $G(t)$ from an infector located in zone i; external sources $C_s(t)$ from the supply of a mechanical ventilation system or $C_j(t)$ from the

infiltration of a neighboring zone; the losses Q_r for the return to the mechanical system, Q_{lx} from the local exhaust such as an exhaust fan, Q_{ac} from an air cleaner, Q_{UVr} from an in-room GUV device, Q_{dep} from the particle deposition, Q_{dec} from the virus infectivity decay/inactivation process, and Q_{exf} from the exfiltration to neighboring zones. The loss rates are expressed as a volumetric flow rates [m^3/s]. Note that Q_{UVr}, Q_{dep}, Q_{dec} are not actually flow rates, but are expressed as equivalent flow rates, as if it was a loss due to ventilation. A ductwork filter, such as a MERV-rated filter (i.e., η_{MERV}) and a duct GUV device (i.e., η_{UVd}) contribute to lowering the supply concentration level $C_s(t)$ of the mechanical ventilation system (Eq. (2)).

The impacts of mask wearing are evaluated in terms of the mask efficiency M_{exh} for the exhalation of the infector in Eq. (1), and M_{inh} for the inhalation of the susceptible in the exposure equation Eq. (3). For a given exposure time duration from t_1 to t_2, Eq. (3) estimates the susceptible's number of inhaled quanta (n_q) at a breathing rate B with probability of mask wearing F_m, given the airborne particle concentration in the space $C_i(t)$ as calculated by Eq. (1). The exposure particle counts are then used as the input for the estimation of infection risk.

$$V\frac{dC_i}{dt} = (1-M_{exh})G(t) + Q_sC_s(t) + \sum_{j=1}^{n} Q_{\mathrm{inf,\,j}}C_j(t) - \left(Q_r + Q_{lx} + \eta_{ac}Q_{ac} + Q_{UVr} + \sum_{k=1}^{s} Q_{\mathrm{dep,\,k}} + Q_{dec} + \sum_{j=1}^{n} Q_{\mathrm{exf,\,j}}\right)C_i(t) \quad (1)$$

M_{exh} = mask exhale efficiency, which was assumed to be the same for all particle sizes;
G = virus generation rate [*quanta*/s]; in this study a constant generation rate was used, however G can be set to vary in time in CONTAM [27];
η = filtration efficiency with subscripts: **a**ir **c**leaner, **MERV** filter, and inactivation efficiency of G**UV** light in HVAC **d**uct;
k = deposition surface, which include the wall, floor, ceiling, and other surfaces;
n = number of neighboring zones;
t = time [s].

The number of inhaled quanta n_q can be expressed as:

$$n_q = B(1 - M_{inh} \times F_m)\int_{t_1}^{t_2} C_i(t)dt \quad (3)$$

Where B = breathing rate (m^3/s);
M_{inh} = mask inhale efficiency, which was assumed to be the same for all particle sizes;
F_m = the percentage of mask wearing;

To compare the relative significance of each term, Eqs. (1)–(2) are non-dimensionalized by $G(t)$:

$$\frac{V}{G(t)}\frac{dC_i}{dt} = 1 - M_{exh} + \frac{1}{G(t)}(1-\eta_{MERV})Q_{rec}C_{rec}(t)(1-\eta_{UVd}) + \frac{1}{G(t)}\sum_{j=1}^{n} Q_{\mathrm{inf,\,j}}C_j(t) - \frac{1}{G(t)}\left[\eta_{ac}Q_{ac} + Q_{UVr} + \sum_{k=1}^{s} Q_{\mathrm{dep,\,k}} + Q_{dec} + \sum_{j=1}^{n} Q_{\mathrm{exf,\,j}} + Q_{lx} + Q_r\right]C_i(t) \quad (4a)$$

Note when $C_{rec} = C_i$

$$\frac{V}{G(t)}\frac{dC_i}{dt} = 1 - M_{exh} + \frac{1}{G(t)}\sum_{j=1}^{n} Q_{\mathrm{inf,\,j}}C_j(t) - \frac{1}{G(t)}\left[\eta_{ac}Q_{ac} + Q_{UVr} + \sum_{k=1}^{s} Q_{\mathrm{dep,\,k}} + Q_{dec} + \sum_{j=1}^{n} Q_{\mathrm{exf,\,j}} + Q_{lx} + Q_{exh} + \eta_{MERV}Q_{rec} - (1-\eta_{MERV})\eta_{UVd}Q_{rec}\right]C_i(t) \quad (4b)$$

$$Q_sC_s(t) = \left[(1-\eta_{MERV})Q_{rec}C_{rec}(t) + Q_{oa}C_{oa}(t)\right](1-\eta_{UVd}) \quad (2a)$$

The outdoor air concentration, C_{oa}, is usually zero in this context, so:

$$Q_sC_s(t) = (1-\eta_{MERV})Q_{rec}C_{rec}(t)(1-\eta_{UVd}) \quad (2b)$$

Where: V = zone volume [m^3];

Q = volumetric flow rate [m^3/s] with subscripts: **s**upply, **r**eturn, **l**ocal e**x**haust, **a**ir **c**leaner, **UV** light in-**r**oom (equivalent), **dep**osition to interior surfaces (equivalent), virus infectivity **dec**ay (equivalent), **inf**iltration from neighbor zone including the ambient, **exf**iltration to neighbor zones including the ambient, **rec**irculation of HVAC system;
C = active virus concentration in the air [quanta/m^3] with the following subscripts: **o**utdoor **a**ir through HVAC system, infectious zone i where the infectious person is located, neighbor zone j, **s**upply, **rec**irculation of HVAC system;

In Eq. (4a), (1 - M_{exh}) is the airborne portion beyond what is removed by the mask (M_{exh} is the efficiency that the mask removes upon exhale), the rest of the terms to the right of the equal sign are the sum of all mitigation contributions to remove this airborne portion. When 1 - M_{exh} + $\sum$(QC/G) = 0, then, the left side of Eq. (4a) will be zero, which means the inhaled quanta concentration will be zero.

In reality, it is often that $C_{rec} < C_i$ because of the mixing in the ductwork and the diluting of the aerosol transport process among different zones. So when virus aerosol reaches the MERV filter, the actual concentration could be lower than that in the source zone. So the efficacy of the centralized duct-level mitigations, e.g., the MERV filter or the in-duct GUV, may decrease with the size of the mechanical system because of the long dilution process during aerosol transport. Thus localized virus aerosol mitigation strategies are preferred compared to the strategies applied in the ductwork, and larger mechanical systems should have more localized solutions inside rooms. Because $C_{rec} < C_i$ in

Table 1
Estimated equivalent removal efficiencies for different mitigation strategies.

Strategy	Masks	Outdoor Air	PAC	MERV Filter	In-Room GUV	In-Duct GUV
Removal efficiency (%)	M	$\frac{Q_{oa}C}{G}$	$\frac{\eta_{ac}Q_{ac}C}{G}$	$\frac{\eta_{MERV}Q_{rec}C}{G}$	$\frac{Q_{UVr}C}{G}$	$\frac{(1-\eta_{MERV})\eta_{UVd}Q_{rec}C}{G}$

reality, Eq. (4b) may overestimate the efficacy of MERV filters and GUV in the ducts.

The above dimensionless equations reveal how different mitigation strategies affect airborne transmission. Of interest is how significant each term is when compared to each other and to the mask efficiency. For an exposure time of Δt, the mask efficiency M is proportional to other building component removal processes generally according to:

$$M \sim \frac{QC}{G} \tag{5}$$

Table 1 details these equivalent removal efficiencies used in a building to reduce the aerosol concentration and thus exposure.

The air mass balance equation is given in Eq. (6) [44]:

$$Q_s + \sum_{j=1}^{n} Q_{\text{inf, j}} = \sum_{j=1}^{n} Q_{\text{exf, j}} + Q_{lx} + Q_r \tag{6}$$

The infiltration, exfiltration, and internal-zonal airflow are modeled by a power law. An example of infiltration from Zone j to Zone i is as shown in Eq. (7) [50].

$$Q_{\text{inf,j}} = \frac{C_D A_L}{1000}\sqrt{\frac{2}{\rho}}(\Delta P_r)^{0.5-n}\Delta P_{j,i}^{n} \tag{7}$$

C_D = flow discharge coefficient; A_L = leakage area, m^2; ρ = air density, kg/m^3; ΔP_r = reference pressure difference, Pa; $\Delta P_{j,i}$ = pressure difference between zone j and zone i, Pa; and n = flow exponent.

In a CONTAM simulation, the wall leakage is often divided into three portions vertically to represent the leakages at the top edge, middle section, and bottom edge of a wall. The pressure difference includes three components: thermal buoyancy, wind pressure (if applicable), and zone pressure differences due to HVAC operations. The thermal buoyancy component is a function of the zone temperature difference as defined by users (or from an energy simulation software, such as EnergyPlus [45]). The wind pressure component depends on the local wind pressure coefficient and is a function of local terrain features, building orientation, and reference wind velocity from the weather conditions. In this study, the well-mixed assumption of air was made without considering turbulent mixing of airflows in zones. However, in the real world, occupants' activities and heat sources may all interrupt airflow patterns in the room, exerting an influence on zonal infiltrations. This could be investigated in future studies using the CFD capabilities of CONTAM [51,52].

2.3. Airborne infectious risk estimation

This study developed an approach, which is named "CONTAM-*quanta*", to enable the CONTAM model to estimate airborne virus transmission in terms of quanta and calculate the probability of infection for SARS-CoV-2. The concept of quanta for airborne transmission, a hypothetical infectious dose unit, was first proposed by Wells in 1955 [53]. A *quantum* was defined as the inhaled dose needed to infect a person. The number of infected occupants bears a Poisson relation to the number of quanta they breathe, which means 63% of occupants will be infected when each occupant breathes one quantum on average. This relationship is widely known as the Wells-Riley equation [29], which is expressed as follows:

$$P = \frac{N_c}{N_s} = 1 - e^{-n_q} \tag{8}$$

where P = the probability of infection, also known as the individual exposure risk [14], N_c = the number of infection cases, N_s = the number of susceptible.

The number of quanta inhaled n_q (quanta) was expressed in Eq. (3).

Modeling is often challenged by the uncertainties in the input parameters. So although this paper reports the quanta concentrations in different zones of a building, we recommend the risk estimation and the comparison of different risk mitigation strategies be conducted on a relative basis. The proposed CONTAM-*quanta* approach was verified by comparing the predicted numerical results to those from the literature. The details can be found in Appendix 1.

A few studies have investigated the quanta emission rate of SARS-CoV-2 [28,34]. Buonanno et al. [14] proposed an approach that provided a range of estimates for different infection scenarios. Here are some assumptions used in this evaluation approach: Firstly, the air in the room was assumed to be well-mixed. In addition, this study assumed a generation rate for loud speaking of 65 quanta per hour and one infector in the source zone. Detailed assumptions for the investigated scenario are described in the next section. We also assumed a quanta deposition rate of 0.3 h^{-1} estimated by Thatcher et al. [69] for particles from 0.55 to 1.54 μm in diameter, and a quanta deactivation rate for SARS-CoV-2 of 0.63 h^{-1} [54]. The removal efficiency of air cleaning using filtration that mechanically removes particles from an air stream depends on the size of the particles being cleaned. This study used efficiencies for particle sizes between 1 μm and 3 μm [55]. Minimum efficiency values were adopted for conservative estimation. The MERV filter efficiency in the CONTAM simulation was then determined using [56]. For example, for the MERV8 filter, its quanta removal efficiency was 20%. The HEPA filter efficiency in the PAC was 99% [57]. It is also possible to use CONTAM with removal/deposition rates as a function of particle size. The maximum building occupancy was based on the corresponding EnergyPlus prototype building [58,59]. The total number of occupants was divided into infectors and susceptibles. Infectors were individuals who could generate "quanta" in the building, and the number of susceptibles was equal to total occupancy allowed in the building minus the number of infectors.

To determine the acceptable level for individual exposure risk from a public health perspective in which outbreaks need to be minimized, the basic reproduction number R_0 was used. The basic reproduction number is defined as the expected secondary infections (N_c) caused by a typical infector (I) among a completely susceptible population ($R_0 = N_c/I$) [60]. Wells' study of airborne spread of measles in an elementary school in 1978 also used this approach. When $R_0 > 1$, the virus may spread in the population [29], so the target exposure risk level was set to $R_0 < 1$. This metric has also been applied in other studies [28,34,60], including a study tracing airborne SARS-CoV-2 transmission in public buses and subway trains [61]. Note that because of the uncertainties of the model, $R_0 > 1$ does not imply there will be a 100% chance of infection. From the probability point of view, it should be interpreted on a relative basis; for example, a lower R_0 means less chance of the community virus transmission or vice versa.

3. Case study – US DOE large office prototype building

3.1. Simulation model and inputs

The US DOE prototype commercial building models were created to assess building energy efficiency measures and the development of

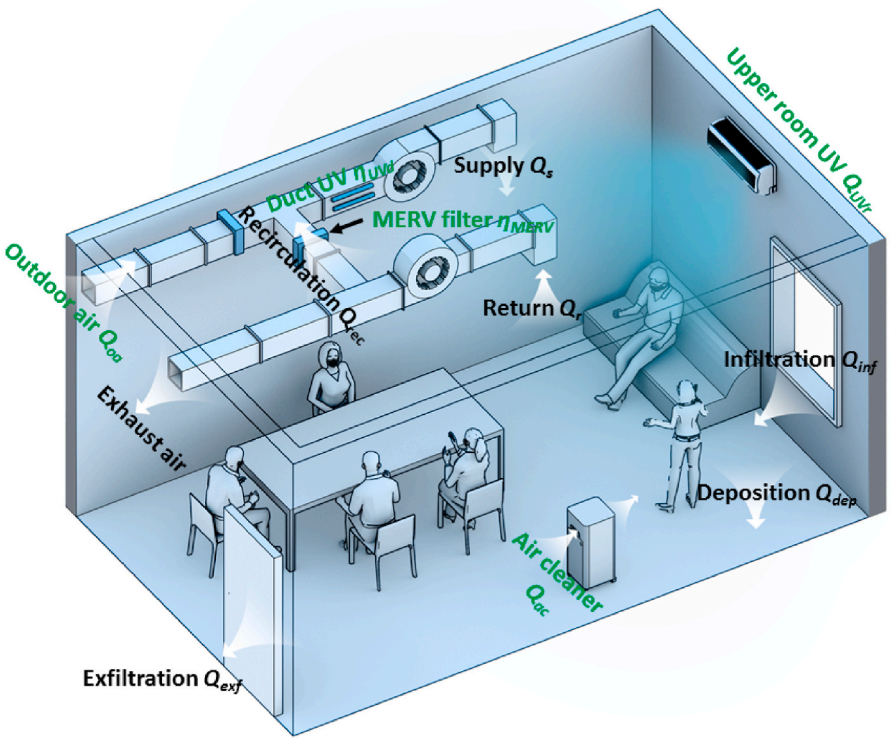

Fig. 1. Schematic of airborne transmission routes.

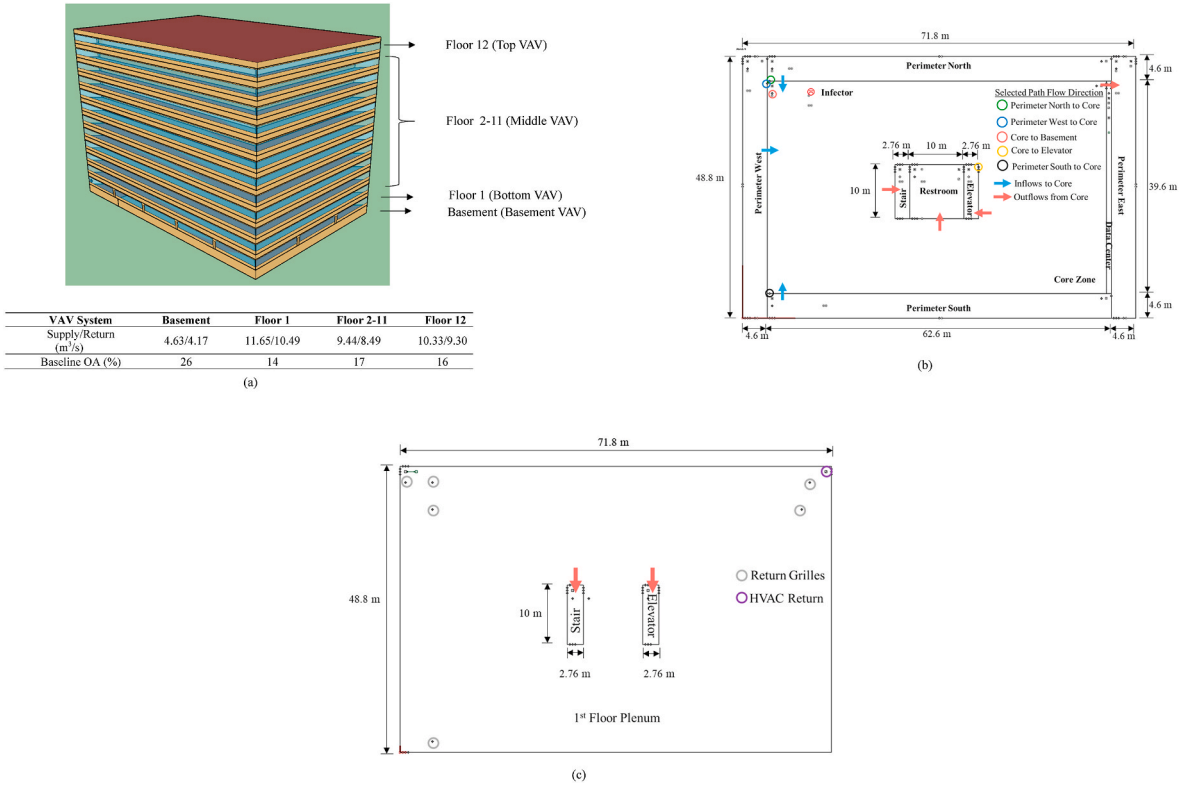

VAV System	Basement	Floor 1	Floor 2-11	Floor 12
Supply/Return (m^3/s)	4.63/4.17	11.65/10.49	9.44/8.49	10.33/9.30
Baseline OA (%)	26	14	17	16

Fig. 2. (a) Drawing of the DOE large office prototype building with ventilation air flow rates and outdoor air percentage; (b) CONTAM model schematic of the 1st-floor; and (c) drawing of the 1st -floor plenum with the return grille and HVAC return [64].

energy standards and codes. Sixteen prototype building types were developed to represent 70% of the commercial building stock [58]. The corresponding CONTAM models of these DOE prototype building models were later created for building ventilation and IAQ analysis [62]. Building parameters such as ventilation, occupancy, and building envelope airtightness were defined following the *ASHRAE Standard*

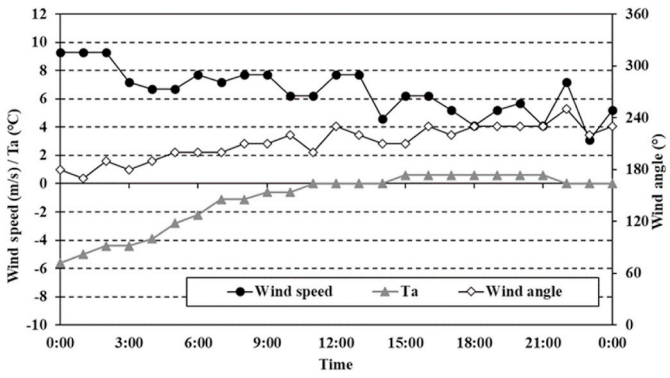

Fig. 3. Weather parameters for Chicago (December 21st) used in simulations [58].

90.1-2013 [63] and *ASHRAE Standard 62.1-2013* [59]. The airflow paths and possible mitigation strategies are illustrated in Fig. 1. This study chose the large office prototype building model to demonstrate the CONTAM-*quanta* approach (Fig. 2).

The building has 12 floors, footprint of 3563 m^2, one basement, and a flat roof. Except the basement, each floor has a central core zone (2324 m^2) with one staircase, elevator (and shaft), and restroom located in the middle of the zone, a data center, and the perimeter zones in four directions. The height from floor to ceiling is 2.74 m and the floor-to-floor height is 4.0 m because of the additional height of the plenum on each floor. Each floor is connected to the top and bottom floors through the staircase and elevator shafts and floor/ceiling leakages, and to the ceiling plenum through one return grill of each zone. Internal wall leakages between every two zones are defined as the three leakage paths at the top, middle and bottom locations. Large internal leakage paths are important and include the leakage path between each perimeter zone and the core zone (as shown by the colored circles in Fig. 2b), which is 50% of the wall area; the leakage paths between the restroom (transfer grille), staircase, elevator shaft and the core zone (as shown by the arrows in Fig. 2b); and a leakage path representing the return air grill from the core zone to the plenum.

The HVAC system includes four individual variable-air-volume (VAV) systems serving the basement, the 1st floor, the 2nd–11th floors, and the 12th floor as shown in Fig. 2a with different supply, return and outdoor air (OA) rates. The total return was set to 90% of supply to achieve the common design goal of pressurizing commercial buildings in CONTAM [62].

The simulations were conducted for one weekday, a Typical Meteorological Year version3 (TMY3) weather winter design day (December 21st), in Chicago, with the hourly weather in Fig. 3. Each floor was assumed to have 134 occupants in each core zone. One infected person was assumed to be in the 1st floor core during working hours (8:00–17:00) without leaving the space. The assumption that the infected person did not leave the building was probably the worst-case scenario with the highest exposure risk. The core zone was selected because typically most of the office staff stay here during working hours. The first floor was chosen as vertical transmission risks exist in the elevator shaft and stairs (Fig. 7). Vertical transmission evidence for the SARS-CoV-2 has been previously reported [36]. The VAV system started at 6:00 and turned off at 22:00. The CONTAM model was created to match the operation and occupancy schedules of the EnergyPlus model. The maximum design flow rates determined by the EnergyPlus simulation were used as inputs for the HVAC supply rates in the CONTAM model [65].

Table 2 summarizes the key simulation parameters used in this study. The effectiveness of different strategies on mitigating virus aerosol exposure risks was investigated, including increasing outdoor air ventilation rates, equipping the building with air-cleaning devices such as MERV filters, PACs with HEPA filters, and in-room/in-duct GUV, and layering with personal mask wearing. The baseline OA rate from the DOE prototype building model (see the table in Fig. 2a) with a MERV8 filter was defined as the baseline (BL) case "MERV8 + BL"; whereas the total supply and return flow rates of the VAV systems were kept the same for all strategies.

3.2. Simulation results

3.2.1. Room-to-room quanta transmissions and exposure risks

The multizone analysis starts with understanding how the airflow

Table 2
Input parameters for the CONTAM-*quanta* simulation of the DOE large office prototype building 1st-floor core zone.

Inputs			Parameters	References
Zone geometry	Volume (m^3)/Area (m^2)	Core	6376/2324	[65]
		Perimeter West (Perimeter East)	608/224.5	
		Perimeter North (Perimeter South)	803/288	
		Restroom	277/100	
		Stairs (Elevator Shaft)	75.7/27.6	
		Data Center	98.6/36.0	
Zone occupancy	Infector		1	–
	Susceptibles		133	[65]
Initial quanta concentration	Concentration (quanta/m^3)		0	–
Quanta generation	Quanta generation rate (quanta/h)		65	[14]
	Breathing rate (m^3/h)		0.72	[66]
	Generation duration		8:00–17:00 (9 h)	–
Deposition and deactivation	Surface deposition rate		0.3 h^{-1}	[67,68]
	Viral particle deactivation rate		0.63 h^{-1}	[69]
Germicidal	in-room GUV removal rate		4 h^{-1}	[70]
Ultraviolet light	in-duct GUV removal efficiency		87%	[71]
	MERV8 removal efficiency		20%	[56]
MERV removal	MERV11 removal efficiency		65%	[56]
	MERV13 removal efficiency		85%	[56]
PAC airflow rates	PAC1		0.46 m^3/s (975 CFM)	From manufacturer
	PAC2		1 m^3/s (2140 CFM)	
	PAC3		1.45 m^3/s (3075 CFM)	
	PAC4		17 m^3/s (36,000 CFM)	
	HEPA removal efficiency		99%	[57]
Mask	Mask wearing percentage		0 or 100%	–
	Exhale removal efficiency		50%	[72]
	Inhale removal efficiency		30%	

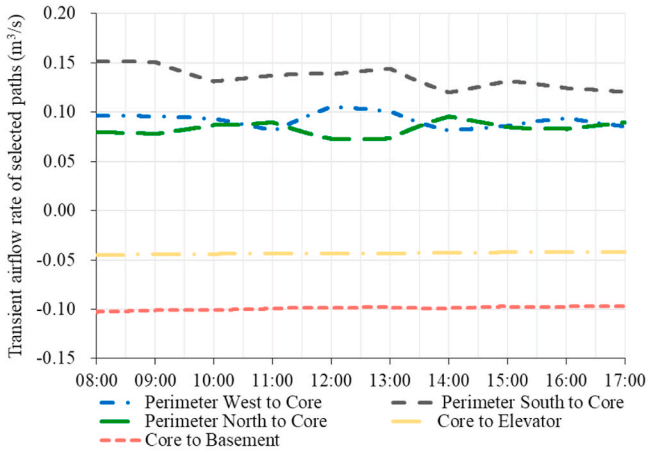

(a)

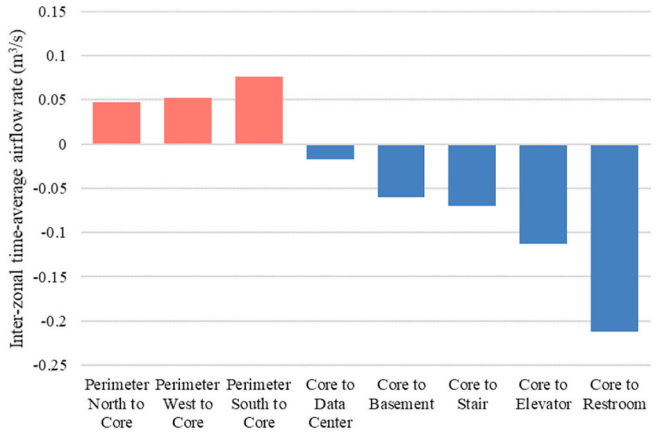

(b)

Fig. 4. (a) Transient airflow rates for selected paths (positive values indicate airflows into the Core Zone, negative values indicate airflows out of the Core Zone); (b) average internal-zonal airflow rates. The zone locations can be found in Fig. 2.

patterns on the same floor for the baseline case (MERV8+BL), (i.e., inter-zonal airflows between the core zone and the neighbor zones) impact room-to-room quanta transmission. The ambient environmental conditions and the operation of HVAC systems impact the zonal airflows. Fig. 4a illustrates the transient airflows for the five paths (Fig. 2b) on the 1st floor with the positive values for the inflows to the core zone. The airflow of the Perimeter South zone varies the most, whereas other flows are more stable throughout the day. The inter-zonal outflows tend to be relatively more steady than the inflows, which were more subject to the ambient conditions because they were connected to the perimeter zones. Fig. 4b shows the 9-h average inter-zonal total airflow rates between two zones of the 1st floor: the average of the summation of all airflow paths between the two zones with the airflow directions indicated by the arrows (Fig. 4b). Although the HVAC system pressurizes the building during the winter (the return is 90% of the supply as shown by Fig. 2a, three zones (Perimeter North, Perimeter West, and Perimeter South) all have the inflows to the Core Zone as a result of the dominating wind direction of the day of 180° ~ 240° (Southwest winds) and 4–8 m/s. The outflows from the Core Zone to the Restroom, Elevator shaft, and Stair were significantly higher than other paths due to the combined impacts of the pressurization of the HVAC system and the stack effects in these spaces. The Restroom is even more underpressurized due to an exhaust fan operating from 6:00 to 22:00 at 0.15 m^3/s. Another potential transmission route is the return grilles at the ceiling of the 1st floor to the plenum (Fig. 2c). Because all return airflows go through the plenume return grilles back to the VAV systems, the leakages in the plenum also potentially contribute to airborne transmision to the stairs and the elevator shafts as indicated by the airflow directions in Fig. 2c. This would result in potential floor-floor transmissions through these vertical spaces.

Fig. 5a reports the simulated transient quanta concentrations in all zones of the 1st floor when the infector was located in the 1st-floor Core Zone (Fig. 2b). For the baseline case (MERV8+BL OA), during the initial two h (8:00–10:00), the quanta concentration accumulated in the zones rapidly; it reached steady state after 10:00. The average quanta concentration in the Core zone was more than twice the levels of other zones except for the Restroom, which has the 2nd highest quanta level. It is because that one return grille was installed in the Restroom to balance airflows in the building. Fig. 5b shows the accumulated individual exposure risk for an occupant in different zones on the 1st floor over the working hours. At the end of the nine working hours, the infection risk is less than 2% in the Core Zone, 1.6% in the Restroom, about 1% in the Elevator shaft, Stair and Datacenter, and less than 0.7% in all other ones of the 1st floor.

Fig. 5c explains the fate of all the airborne quanta at the end of working hours on the 1st floor. More than half of the airborne quanta (57%) stays in the source zone (Core). Because all air returns to the VAV system through the plenum, this explains the non-zero concentration levels in the Perimeter North, West and South despite only inflows from these zones to the Core Zone. In other words, these quanta concentrations mostly come from the return air from the Core Zone through the VAV system. This shows that a poorly-balanced pressure distribution could create potential inter-zonal transmission risks. Thus, it is preferred to avoid spaces with intensively negative pressures, preventing the possible transmission risk. In summary, the room-room transmission routes in the 1st floor were: Core→Restroom through the restroom return grill; Core→Staircase and Core→Elevator shaft through leakage paths; Core→Data Center through internal partition path; and Core→Perimeter Zones through the plenum returns.

3.2.2. *Floor-floor quanta transmissions and exposure risks*

The HVAC pressurization and stack effect in the staircase and elevator shafts could contribute to floor-floor transmission, but the 1st floor ventilation does not because it has its own individual VAV system. Here, for the baseline case (MERV8+BL OA), we report the relative exposure risks of all zones in the building compared to the risk in the 1st-floor Core Zone when the infected person is in the 1st-floor Core Zone (i.e., $P_{floor\text{-}zone}/P_{1st\text{-}Core}$) in Fig. 6. At the 1st floor, the 1st-floor Core Zone has the highest exposure risk, followed by the Restroom, Elevator Shaft and Stair. The "Elevator" discussed in this study refers to the elevator shaft in the building. On the higher floors, the elevator shaft and stair are the most infective zones. Noteably, at the 7th floor, the Core and Restroom zones' risks start to increase and the 12th floor risk gets a suprising rebound.

The above observations may be explaind by the pressure profiles in the stairs and elevator shaft as shown by Fig. 7. Higher risks of the elevator shaft than that of stairs at the lower floors (<the 4th floor) can be explained by their higher inflows to the elevator shaft (Fig. 4b) and the stronger stack effect than the stairs (Fig. 7). However, the elevator shaft risks continuously decrease with the height because the stronger stack effect tends to drive more non-polluted air from the neighbor zones

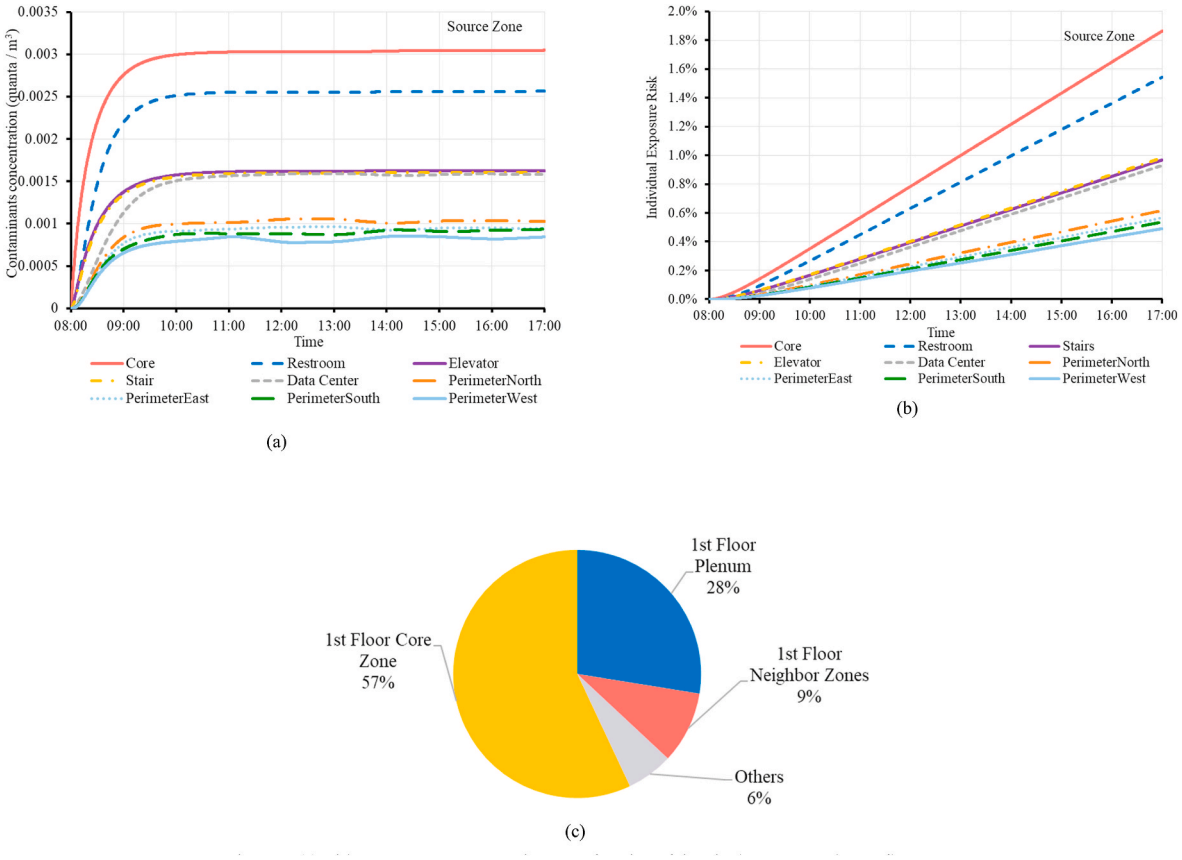

Fig. 5. (a) Airborne quanta concentrations as a function of time in the zones on the 1st floor; (b) transient exposure risks for an occupant in the zones of the 1st floor; and (c) airborne quanta distribution on the 1st floor.

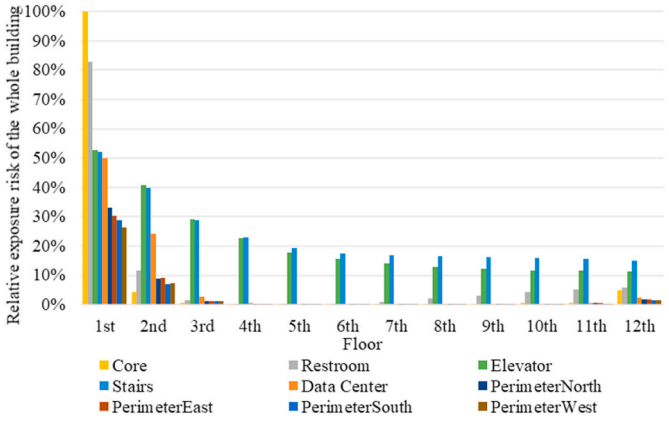

Fig. 6. Relative risks of all zones compared to the 1st-floor zones ($P_{floor}/P_{1st\text{-}Core}$ x 100%).

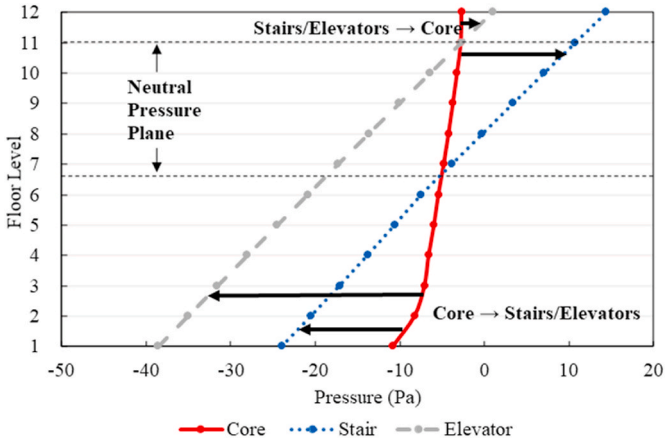

Fig. 7. Average pressure profiles of the Core Zones, Stairs and Elevator shaft.

into the elevator shaft, thus helping to dilute the space. This continues until the 7th floor, where the airflow from the stairs starts to enter the Core Zones carrying the airborne quanta because the neutral pressure plane (NPP) of the stairs is established above the 6th floor. This explains why the restrooms above the 6th floor have non-zero risks. The elevator shaft NPP forms on the 11th floor, above which the airborne quanta of both the stairs and elevator shaft starts to infiltrate to the 12th floor. As a result, the Core Zone and Restroom of the 12th floor have higher risks than lower floors. These results show that the floor-floor transmission is possible as a result of the dynamics of pressure distributions in a whole building, and higher floors could become vulnerable due to the combined impacts of the stack effects and pressurization of the HVAC systems. To compare the multizone to the single-zone analysis futher, Appendix 2 discusses the difference between the CONTAM-quanta approach and other single-zone models (i.e., COVID19 Estimator, REHVA calculator, FaTIMA), and multizone models (i.e., CONTAM

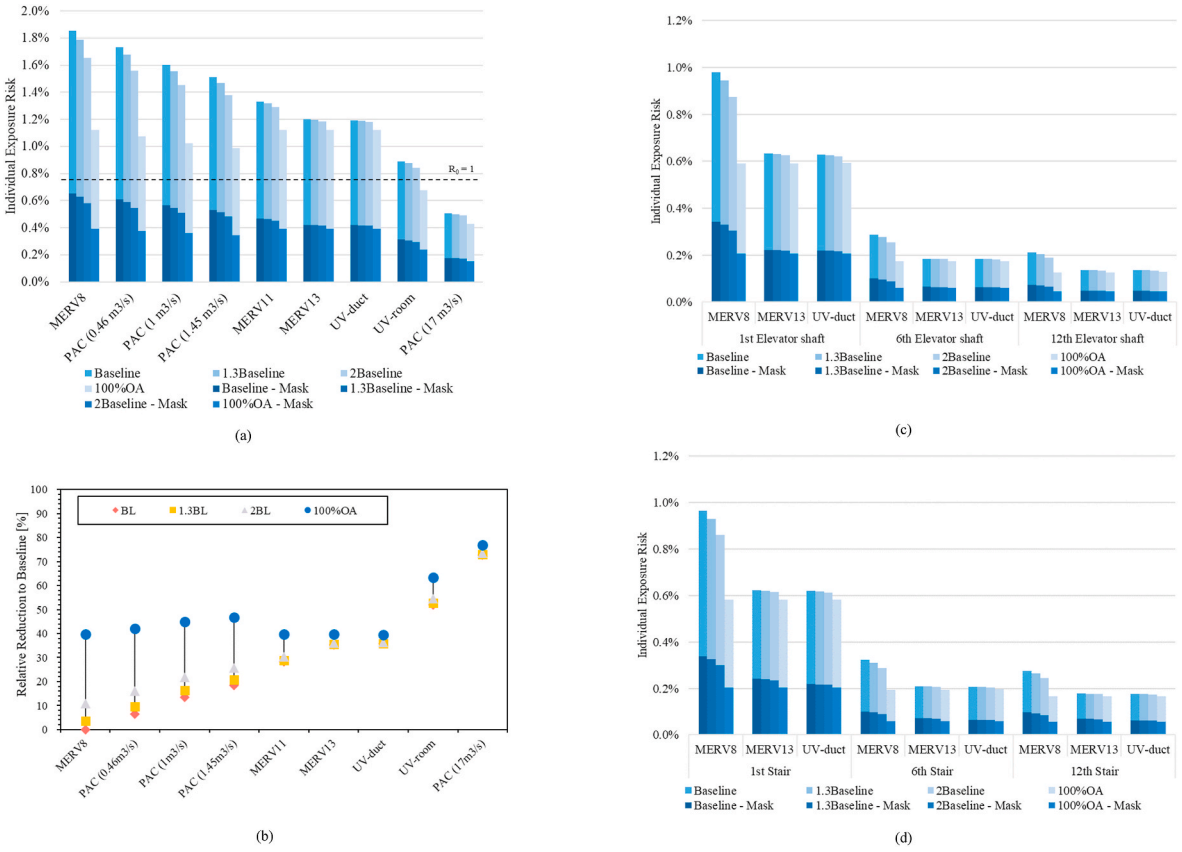

Fig. 8. (a) Individual exposure risks in the 1st floor core zone under different combined mitigation strategies; (b) relative risk reduction compared to the baseline case (the baseline case is denoted by the red dot). Each line is for a different OA rate. As mitigation strategies are adopted the relative risk reduction increases; (c) Individual exposure risks in elevator shafts under different mitigations (1st, 6th and 12th floor); (d) Individual exposure risks in the stairs under different mitigations (1st, 6th and 12th floor). (For interpretation of the references to color in this figure legend, the reader is referred to the Web version of this article.)

without the *quanta* approach).

3.2.3. *Mitigations of exposure risk*

The previous analysis shows that the most vulnerable space is where the infective source is located (1st-floor Core Zone), which is also the most populated. Therefore, the following risk mitigation analysis is focused on this zone. The results of predicted exposure risks for the occupants' nine-h exposures in the 1st-floor Core Zone are demonstrated in Fig. 8a. The acceptable risk level ($R_0 = 1$) was calculated to be 0.75% for this zone. For the baseline case, the exposure risk was estimated to be 1.83% without mask wearing. By increasing the OA rate to 1.3BL, 2BL or 100% fresh air, the exposure risk would drop to 1.79%, 1.66%, and 1.12%, respectively. The upgrade of the MERV8 filter to a MERV11 or MERV13 reduces the risk to 1.30% and 1.22%. Adding germicidal GUV, the in-duct GUV would decrease the baseline exposure risk to 1.19%, while the room GUV could lower the risk to 0.89%. In addition, adding PACs would also contribute to effective mitigation. The use of PACs with recirculating airflow rates of 0.46 m^3/s (PAC1, 0.71 ACH), 1 m^3/s (PAC2, 1.55 ACH) and 1.45 m^3/s (PAC3, 2.25 ACH) would reduce the exposure risks to 1.73%, 1.60% and 1.51%, respectively. The air cleaner with the highest flow rate of 17 m^3/s (PAC4, 26.3 ACH) would help limit the risk to 0.51%, achieving an acceptable risk level (0.75%). The performance of PAC4 was based on a large-capacity prototype air cleaner that had been developed by this study's industrial partner. In comparison, wearing masks is the most effective and can keep $R_0 < 1$ for all evaluated mitigation strategies.

It should be noted that the risk estimation was conducted mainly for comparing different mitigation strategies. For each of the mitigation strategies, the relative risk reduction compared to the baseline is shown in Fig. 8b. Upgrading the MERV filters from MERV8 to MERV11 and MERV13 tend to be more effective than adding PACs (PAC1 to PAC3, from 0.46 m^3/s to 1.45 m^3/s). The use of MERV13 and in-duct germicidal UV with the Baseline OA provides similar performance to that of 100% OA. When the 100% OA strategy (the blue dot in Fig. 8b) is adopted, the most relative reduction compared to baseline that can be achieved is 40%; to reduce the risk even further, in-zone strategies need to be adopted also such as operating PACs or in-room GUV.

Infection risk and the impact of duct mitigation strategies (MERV filters and in-duct GUV) for the elevator shaft and stairs were also investigated, and results are shown in Fig. 8c and Fig. 8d. As shown in Fig. 6, aerosols could transmit through the building via the elevator shaft and stairs. This means that floor-to-floor transmission is possible, and mitigations are needed. MERV13 and GUV-in-duct were effective mitigations, leading to an average of 30% risk reduction in the elevator shaft. This suggests that mitigations in the HVAC ducts of the building not only reduce risks in the source zone but also play a significant role in reducing the transmission between floors.

4. Discussion

For the evaluated mitigation strategies, Fig. 8b shows that doubling outdoor air ventilation did not effectively reduce exposure risks unless

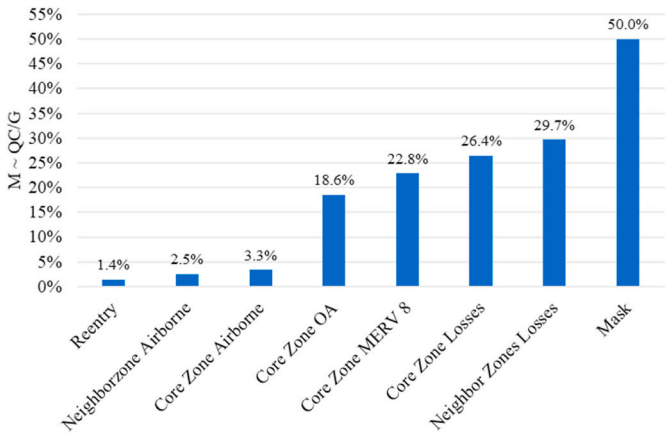

Fig. 9. Comparison of sources and losses of virus aerosol in the large office building core zone to mask efficiency (M ~ QC/G).

100% OA was applied. When the outdoor air percentage was adopted as 100%, the exposure risk was reduced to 1.12%, 40% down from the baseline case. However, operating the HVAC system with 100% fresh air raises concerns over energy cost and thermal comfort indoors. It is relatively difficult to implement high OA ventilation rates in many existing systems. In reality, some existing buildings implemented a "Pandemic Mode" operation by increasing OA rates 1.3–2 times the baseline ventilation rates. In the current study, the analysis shows that the relative reduction in risk achieved by increasing OA flow rates by 1.3 or 2 were minimal when compared to other strategies.

Other active mitigation strategies should be implemented to reduce the risk level further, for example, retrofits that include upgrading MERV filters, and/or adding PACs or germicidal UV lights into the building zones. In this study, three types of MERV filters were investigated: MERV8, MERV11, and MERV13. Results show that upgrading from MERV8 to MERV11 reduced substantially individual exposure risks. For the baseline outdoor air ventilation scenarios, exposure risks fell by 29% for MERV11 and 36% for MERV13. Thus, upgrading MERV filters is effective, though a trade-off between risk mitigation and economic cost needs to be considered due to the elevated pressure drops with higher MERV filters. In the large office building of this study, a MERV11 upgrade combined with other measures, e.g., PAC and germicidal UV, was effective at achieving the desired risk reduction.

Adding PACs or in-room GUV increased the total equivalent air change rate to the Core Zone without interfering with the existing HVAC system operation. The portable air cleaners evaluated in this study covered a large range of capacity, from 0.5 to 42.5 m^3/s, which were based on the information provided by the industrial collaborator. These PACs were equipped with filters with an assumed *single-pass efficiency* of 99%. Among the investigated products, it was found that large capacity PACs (>17 m^3/s) effectively lowered exposure risks below $R_0 < 1$. Thus, the capacity of the PAC should fit the room size; for large volume areas, large capacity PACs or multiple small capacity PACs can be considered. Similar observations also apply to the GUV devices: in-room GUV in general performed better than the in-duct GUV devices in the current study.

Multizone modeling also enables an in-depth analysis of the sources and losses of viral aerosol in the core zone. The parameter $\frac{QC}{G}$ (Eq. (5)) is compared to the efficacy of masking (M in Eq. (5)) to better understand whole building mitigation strategies compared to individual strategies and to sources. The comparison is reasonable because mask wearing is commonly recognized as one of the most effective risk reduction strategies and thus can be used as a baseline for evaluating the risk mitigation efficacy; it however relies on the individual to wear a mask compared to the building strategy that relies on building systems design and operation. This is achieved by summing the airflows, Q, and time-dependent zone concentrations, C, for all components as illustrated by Eq. (4b). Fig. 9 shows that the "Reentry" (Aerosols re-entering the Core Zone from neighboring zones) was 1.4%. This means that 1.4% of all generated quanta re-entered the Core Zone. Much of the generated airborne quanta stayed in the Core Zone (3.3%), and 2.5% remained in all the neighboring zones. The baseline OA rates flushed 18.6% of all generated, and for MERV8 filter, it filtrated 22.8%. The "Core Zone Losses" and "Neighbor Zone Losses", which include the virus' natural inactivation, deposition, and exfiltration in the Core Zone and all neighbor zones, contributed to a loss of 26.4% and 29.7% of all generated quanta, respectively. As a comparison, if mask wearing was enforced, the most effective reduction would be 50%, which is the typical efficiency value for a mask [26]. Therefore, Fig. 9 shows that mask wearing would be more effective than the combined effects of the baseline OA and MERV 8 in this case study. In addition, it also shows that although there may be inter-zonal spreading in the building, the losses in the neighbor zones would also be high.

For all evaluations in this study, the air within the zones was assumed to be well-mixed. However, this assumption may simplify the real exposures in buildings. There could be additional turbulent mixing that happens within and between internal zones in the building due to heat sources, movement of occupants, flows created by doors opening, etc. Differential exposure risks for individuals at different locations in the zone could be considered in future studies by utilizing the CFD capabilities of CONTAM [51,52].

Office environments are often crowded, poorly ventilated places where staff share the space for prolonged working hours. It has been reported that work environments are one of the most common venues for SARS-CoV-2 transmission [73]. An epidemiological investigation of a superspreading event in an open-plan office in Switzerland found that one index person in the office directly infected 67–83% of the team members [74]. In another study conducted in England, the attack rate was reported to be 55% in a public-facing office [75]. Though the events, office configurations and room ventilation conditions varied, these evaluations suggest that, in real working situations, the transmission risks could be high. Infected cases reported by these studies not only worked at their desks, but also attended meetings in conference rooms during working hours.

Prateek et al. used steady-state simulations showing that stairwells can potentially experience higher aerosol concentrations than other conditioned zones of an office building [40]. In our study, exposure risks in stairs and elevator shafts of the large office building were also found to be higher than that for perimeter zones and the data center (Fig. 5a). This suggests that virus-laden aerosol could transmit to stair and elevator shafts, where mitigations such as PACs and GUV lights should be considered. Jensen evaluated the effect of integrated IAQ strategies (source control, ventilation, and air cleaning) on reducing infection risks in open-plan offices [31]. In this evaluation, a risk reduction factor (RRF) was estimated for each of the strategies such as doubling the ventilation, adding semi-open partitions *etc*. Compared with the RRF, this study provides a more precise quantification of cleaning performance for mitigation strategies and enables a reasonable comparison. In another assessment of laboratory and office environments of SARS-CoV-2 transmission, the typical office room (two air exchanges per hour) was suggested to be at least vacant for 2.5 h [76]. However, the assessment of pre-flush strategies was not included in this study, and it can be investigated in the future.

Though the approach proposed by this study could serve as an effective way for designing mitigation strategies in buildings, uncertainties cannot be avoided in risk assessments. The classic Wells-Riley model has been used to evaluate airborne exposure risks since the 1970s [29], helping the public understand airborne infection risks. However, the accurate estimation of the "quanta" generation rate remains unclear, although great efforts have been made to understand the quanta generation rate for SARS-CoV-2 under different conditions. Uncertainties in estimated input parameters can also contribute to the variation in risk

estimation, such as breathing rates, filter efficiency, GUV inactivation efficiency, mask inhale/exhale efficiency, and other key parameters. Therefore, uncertainties and the stochastic nature of the input parameters could be included in future studies, such as was done in the Skagit Valley Chorale Outbreak study [54].

5. Conclusions

Under the health threats posed by the SARS-CoV-2 virus and, in particular, its highly infectious variants, aerosol transmission indoors must be addressed. Engineering control strategies can improve the indoor air quality in a building. To assess what strategy is most effective, a modeling approach was derived in this study that could be applied to many different building types and an analysis was undertaken to comprehensively compared mitigation strategies for a DOE prototype office building. The modeling approach described by this study allows for an evaluation of the whole-building as a multizoned structure, and the effectiveness of ventilation and air-cleaning components in the building could be effectively evaluated and compared. The large office scenario simulated in this study served as a good example for implementing mitigation strategies. For the baseline case, the zone-to-zone and floor-to-floor spread were possible though the risk was significantly lower in all zones compared to the source zone. The use of a duct-treatment strategy could approach the effectiveness of 100% outdoor air, and adding room cleaning devices such as portable air cleaners and in-room GUV light could further enhance the air cleaning. More building types could be analyzed in future studies.

This study demonstrates how the multi-zone analysis of a DOE prototype building could be conducted and explained the detailed analysis steps of addressing airflows, pressure profiles, airborne quanta levels, and associated transmission risks. The combined effects of the HVAC system operation (e.g., winter pressurization), stack effect, and the ambient weather conditions could play a significant role in the potential whole building transmission, even to a space far away from the infected space. The single-zone or box-type models cannot achieve this level of understanding because they address the airborne quanta transmission assuming that the whole building is a single zone.

The purpose of this risk analysis was not to predict the absolute level of risk in infection in a building, but rather to compare the relative reduction of risks among different mitigation strategies. The current study focuses on one building type. Building-specific studies are important and should be conducted considering the complexities of different building uses and occupancies. Similar studies can be conducted for other DOE multizone prototype building types, such as hotels, schools, retail stores and hospitals, and with different climate zones. For achieving this purpose, the current study also shares all the input files with detailed settings of the large office prototype building with the community to facilitate future studies.

CRediT authorship contribution statement

Shujie Yan: Writing – original draft, Visualization, Validation, Software, Methodology, Formal analysis, Data curation. **Liangzhu (Leon) Wang:** Writing – original draft, Validation, Supervision, Software, Methodology, Formal analysis. **Michael J. Birnkrant:** Project administration, Funding acquisition, Conceptualization. **John Zhai:** Writing – review & editing, Supervision, Software, Methodology, Conceptualization. **Shelly L. Miller:** Writing – review & editing, Supervision, Software, Project administration, Methodology, Funding acquisition, Conceptualization.

Declaration of competing interest

The authors declare the following financial interests/personal relationships which may be considered as potential competing interests: Shelly L. Miller reports financial support was provided by Carrier Corporation.

Appendix 1. Verification of CONTAM-*quanta* Approach

The CONTAM multizone contaminants transportation simulation has been validated by many previous studies in terms of both airflow/ventilation and pollutant predictions [77,78]. Therefore, this verification focused on applying the CONTAM-*quanta* model to the Skagit Valley Chorale superspreading event [79], and comparing results with those from the COVID-19 Aerosol Transmission Estimator [26]. The single-zone CONTAM case – FaTIMA [48] was used to model the quanta transmission. The verification details are illustrated in Table A1. It should be noted that the FaTIMA tool was not originally designed for modeling aerosols in terms of quanta, instead, it models the transmission of infective particles. In this study, we implemented the proposed CONTAM-*quanta* approach in FaTIMA and verified it in this section. Note a verification is to confirm the accuracy of a numerical approach when compared to the previous analytical approach with the same input parameters. This step is important because it ensures the numerical programming of a software tool is able to reproduce the results in the literature.

The transient airborne concentration predictions are compared as follows. Figure A1 shows that the predicted airborne concentrations agrees well with the values predicted using the formula underlying the COVID19 Aerosol Transmission Estimator [26]. In addition, the final airborne aerosol concentration levels were both at 0.56 quanta/m^3 and exposure risks at the end of the 2.5 h event were predicted to be 88.6%. Thus, the proposed CONTAM-*quanta* approach can provide comparable results on estimating exposure as previous studies.

Table A1
Comparison of CONTAM (FaTIMA)-*quanta* single-zone and COVID19 Aerosol Transmission Estimator [26].

	CONTAM (FaTIMA)-*quanta*		COVID19 Aerosol Transmission Estimator	
Zone volume	810 m^3		810 m^3	
Generation	Number of infectors	1	Number of infectors	1
	Particles/Quanta generation rate	970 quanta/h	Infective person	970 quanta/h
Removal	Supply air rate	567 m^3/h	Ventilation with outside air	0.7 h^{-1}
	Return air rate	567 m^3/h (0.7h^{-1})		
	Exhaust air	567 m^3/h (0.7h^{-1})	Exhaust air	567 m^3/h (0.7h^{-1})
	Air cleaner (Filter)	0	Additional control measures	0
	Surface deposition	0.3 h^{-1}	Surface deposition	0.3 h^{-1}
	Inactivation of the virus	0.63 h^{-1}	Inactivation of the virus	0.63 h^{-1}

CONTAM (FaTIMA)-*quanta*.

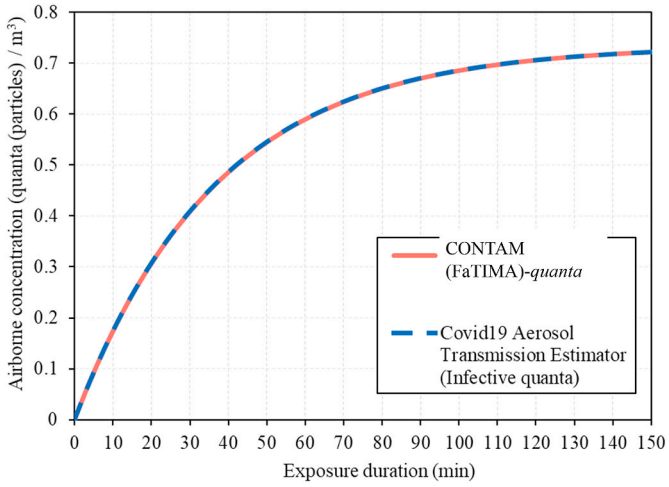

Fig. A1. Transient airborne contaminants concentration predictions during the 2.5h Choir duration (CONTAM-*quanta* vs COVID19 Aerosol Transmission Estimator).

Appendix 2. Comparisons between CONTAM-multizone and FaTIMA-singlezone modeling

The comparisons between CONTAM multizone simulations and singlezone FaTIMA simulations of the baseline case (Baseline OA + MERV8) are illustrated as follows. The differences were due to zone-to-zone transmissions through air leakages and the central ventilation system (VAV in the Large Office). The single-zone FaTIMA only allows steady-state weather conditions while the multizone modeling adopts the Chicago TMY3 weather. The infiltration was also negected by FaTIMA. In CONTAM modeling of the Large Office building, the VAV systems were modeled by a series of air-handling units across different floors, which reflects more realistically the multizone aerosol transmissons, e.g., via return grills. In comparison, one simple supply/return system was applied in FaTIMA. The comparison of the differences is summarized in Table A2 between the proposed CONTAM-*quanta* approach from this study and other single-zone models (i.e., COVID19 Estimator, REHVA calculator, FaTIMA), and multizone model (i.e., CONTAM).

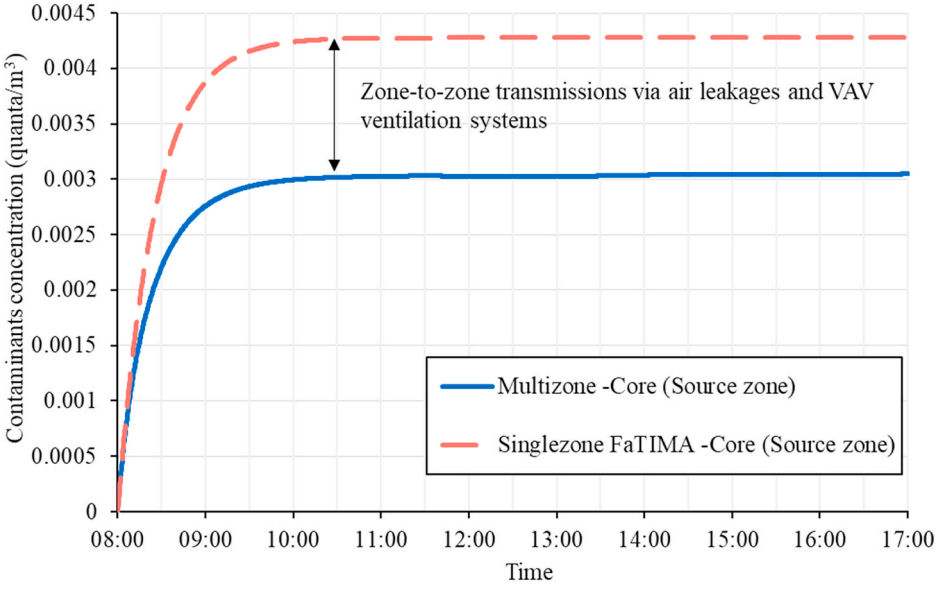

Fig. A2. Comparisons between single-zone and multi-zone simulations of the Large Office.

Table A2
Comparison between different tools for airborne aerosole modeling

	COVID19 Estimator [26]	REHVA calculator [80]	FaTIMA [48]	CONTAM [44]	CONTAM-quanta
Building details	–	–	–	✓	✓
HVAC details	–	–	✓	✓	✓
Occupancy schedule	–	–	–	✓	✓
Weather impacts	–	–	–	✓	✓
Multi-zone analysis	–	–	–	✓	✓
Occupant exposure	✓	✓	✓	✓	✓
Infection risk	✓	✓	–	–	✓

References

[1] WHO, WHO Coronavirus, COVID-19) Dashboard | WHO Coronavirus (COVID-19) Dashboard with Vaccination Data, 2021.
[2] S.S.A. Karim, T. de Oliveira, New SARS-CoV-2 variants — clinical, public health, and vaccine implications. https://doi.org/10.1056/NEJMC2100362, 2021, 1866-1868.
[3] J.P. Moore, P.A. Offit, SARS-CoV-2 vaccines and the growing threat of viral variants, JAMA 325 (2021) 821–822, https://doi.org/10.1001/JAMA.2021.1114.
[4] R.P. Walensky, H.T. Walke, A.S. Fauci, SARS-CoV-2 variants of concern in the United States-challenges and opportunities, JAMA 325 (2021) 1037–1038, https://doi.org/10.1001/JAMA.2021.2294.
[5] Pedroso Rodrigo, C. Hu, Brazil: Covid-19 Caused One in Three Deaths in the Country So Far This Year - CNN, CNN, 2021.
[6] S. Menon, India Covid: How Bad Is the Second Wave? BBC News, 2021.
[7] M. Scudellari, How the pandemic might play out in 2021 and beyond, Nature 584 (2020) 22–25, https://doi.org/10.1038/D41586-020-02278-5.
[8] N. Zhu, D. Zhang, W. Wang, X. Li, B. Yang, J. Song, X. Zhao, B. Huang, W. Shi, R. Lu, P. Niu, F. Zhan, X. Ma, D. Wang, W. Xu, G. Wu, G.F. Gao, W. Tan, A novel coronavirus from patients with pneumonia in China. https://doi.org/10.1056/NEJMOA2001017, 2019, 727-733.
[9] G. Mallach, S.B. Kasloff, T. Kovesi, A. Kumar, R. Kulka, J. Krishnan, B. Robert, M. McGuinty, S. den Otter-Moore, B. Yazji, T. Cutts, Aerosol SARS-CoV-2 in hospitals and long-term care homes during the COVID-19 pandemic, PLoS One 16 (2021), e0258151, https://doi.org/10.1371/journal.pone.0258151.
[10] J.A. Lednicky, M. Lauzardo, M.M. Alam, M.A. Elbadry, C.J. Stephenson, J. C. Gibson, J.G. Morris, Isolation of SARS-CoV-2 from the air in a car driven by a COVID patient with mild illness, Int. J. Infect. Dis. 108 (2021) 212–216, https://doi.org/10.1016/j.ijid.2021.04.063.
[11] J.L. Santarpia, V.L. Herrera, D.N. Rivera, S. Ratnesar-Shumate, S.P. Reid, D. N. Ackerman, P.W. Denton, J.W.S. Martens, Y. Fang, N. Conoan, M. V Callahan, J. V Lawler, D.M. Brett-Major, J.J. Lowe, The size and culturability of patient-generated SARS-CoV-2 aerosol, J. Expo. Sci. Environ. Epidemiol. (2021), https://doi.org/10.1038/s41370-021-00376-8.
[12] J.L. Santarpia, D.N. Rivera, V.L. Herrera, M.J. Morwitzer, H.M. Creager, G. W. Santarpia, K.K. Crown, D.M. Brett-Major, E.R. Schnaubelt, M.J. Broadhurst, J. V Lawler, S.P. Reid, J.J. Lowe, Aerosol and surface contamination of SARS-CoV-2 observed in quarantine and isolation care, Sci. Rep. 10 (2020), 12732, https://doi.org/10.1038/s41598-020-69286-3.
[13] B.U. Lee, Minimum sizes of respiratory particles carrying SARS-CoV-2 and the possibility of aerosol generation, Int. J. Environ. Res. Publ. Health 17 (2020) 1–8, https://doi.org/10.3390/IJERPH17196960.
[14] G. Buonanno, L. Stabile, L. Morawska, Estimation of airborne viral emission: quanta emission rate of SARS-CoV-2 for infection risk assessment, Environ. Int. 141 (2020), https://doi.org/10.1016/j.envint.2020.105794.
[15] L. Morawska, J.W. Tang, W. Bahnfleth, P.M. Bluyssen, A. Boerstra, G. Buonanno, J. Cao, S. Dancer, A. Floto, F. Franchimon, C. Haworth, J. Hogeling, C. Isaxon, J. L. Jimenez, J. Kurnitski, Y. Li, M. Loomans, G. Marks, L.C. Marr, L. Mazzarella, A. K. Melikov, S. Miller, D.K. Milton, W. Nazaroff, P. V Nielsen, C. Noakes, J. Peccia, X. Querol, C. Sekhar, O. Seppänen, S.I. Tanabe, R. Tellier, K.W. Tham, P. Wargocki, A. Wierzbicka, M. Yao, How can airborne transmission of COVID-19 indoors be minimised? Environ. Int. 142 (2020) https://doi.org/10.1016/j.envint.2020.105832.
[16] J.W. Tang, W.P. Bahnfleth, P.M. Bluyssen, G. Buonanno, J.L. Jimenez, J. Kurnitski, Y. Li, S. Miller, C. Sekhar, L. Morawska, L.C. Marr, A.K. Melikov, W.W. Nazaroff, P. V Nielsen, R. Tellier, P. Wargocki, S.J. Dancer, Dismantling myths on the airborne transmission of severe acute respiratory syndrome coronavirus-2 (SARS-CoV-2), J. Hosp. Infect. 110 (2021) 89–96, https://doi.org/10.1016/j.jhin.2020.12.022.
[17] J. Kurnitski, F. Franchimon, J. Hogeling, How to operate and use building services in order to prevent the spread of the coronavirus disease (COVID-19) in workplaces, REHVA 2020 (2020) 8.
[18] ASHRAE, ASHRAE Resources Available to Address COVID-19 Concerns, COVID-19 Prep. Resour, 2020.
[19] M. Guo, P. Xu, T. Xiao, R. He, M. Dai, S.L. Miller, Review and comparison of HVAC operation guidelines in different countries during the COVID-19 pandemic, Build. Environ. 187 (2021), 107368, https://doi.org/10.1016/j.buildenv.2020.107368.
[20] AIVC, AIVC Newsletter, Special Issue COVID-19, AIVC, July 2021 (n.d.).
[21] ASHRAE, GUIDANCE FOR RE-OPENING BUILDINGS, 2021.
[22] ISO/TC 142, ISO 16890-1:2016 Air filters for general ventilation. Technical specifications, requirements and classification system based upon particulate matter efficiency, ePM 1 (2016) 1–27.
[23] INSPQ, COVID-19, Indoor Environment, 2020.
[24] ASHRAE, Ashrae Epidemic Task Force, Healthcare, Ashrae 2021 (2021). https://www.ashrae.org/file library/technical resources/covid-19/ashrae-filtration_disinfection-c19-guidance.pdf.
[25] W. Bahnfleth Phd, Pe, J. Degraw Phd, Reducing airborne infectious aerosol exposure, ASHRAE J. 63 (2021) 18–21. https://lib-ezproxy.concordia.ca/login?qurl=https%3A%2F%2Fwww.proquest.com%2Fscholarly-journals%2Freducing-airborne-infectious-aerosol-exposure%2Fdocview%2F2526333969%2Fse-2%3Faccountid%3D10246.
[26] J. L, , et al.Jimenez, 2020_COVID-19_Aerosol_Transmission_Estimator - Google Sheets, 2020.
[27] Z. Peng, A.L.P. Rojas, E. Kropff, W. Bahnfleth, G. Buonanno, S.J. Dancer, J. Kurnitski, Y. Li, M.G.L.C. Loomans, L.C. Marr, L. Morawska, W. Nazaroff, C. Noakes, X. Querol, C. Sekhar, R. Tellier, T. Greenhalgh, L. Bourouiba, A. Boerstra, J.W. Tang, S.L. Miller, J.L. Jimenez, Practical indicators for risk of airborne transmission in shared indoor environments and their application to COVID-19 outbreaks, Environ. Sci. Technol. 56 (2022) 1125–1137, https://doi.org/10.1021/acs.est.1c06531.
[28] H. Dai, B. Zhao, Association of the infection probability of COVID-19 with ventilation rates in confined spaces, Build. Simulat. 13 (2020) 1321–1327, https://doi.org/10.1007/s12273-020-0703-5.
[29] E.C. Riley, G. Murphy, R.L. Riley, Airborne spread of measles in a suburban elementary school, Am. J. Epidemiol. 107 (1978) 421–432, https://doi.org/10.1093/oxfordjournals.aje.a112560.
[30] J. Lelieveld, F. Helleis, S. Borrmann, Y. Cheng, F. Drewnick, G. Haug, T. Klimach, J. Sciare, H. Su, U. Poeschl, Model Calculations of Aerosol Transmission and Infection Risk of COVID-19 in Indoor Environments, MedRxiv, 2020, https://doi.org/10.1101/2020.09.22.20199489.
[31] J. Zhang, Integrating IAQ control strategies to reduce the risk of asymptomatic SARS CoV-2 infections in classrooms and open plan offices, Sci. Technol. Built Environ. (2020) 1013–1018, https://doi.org/10.1080/23744731.2020.1794499.
[32] C. Sun, Z. Zhai, The efficacy of social distance and ventilation effectiveness in preventing COVID-19 transmission, Sustain. Cities Soc. 62 (2020), https://doi.org/10.1016/j.scs.2020.102390.
[33] A. Katal, L. Leon Wang, M. Albettar, A real-time web tool for monitoring and mitigating indoor airborne COVID-19 transmission risks at city scale, Sustain. Cities Soc. 80 (2022), 103810, https://doi.org/10.1016/j.scs.2022.103810.
[34] J. Shen, M. Kong, B. Dong, M.J. Birnkrant, J. Zhang, A systematic approach to estimating the effectiveness of multi-scale IAQ strategies for reducing the risk of airborne infection of SARS-CoV-2, Build. Environ. 200 (2021), 107926, https://doi.org/10.1016/j.buildenv.2021.107926.
[35] M.-E. Dubuis, J. Degois, M. Veillette, N. Turgeon, B. Paquet-Bolduc, G. Boivin, C. Duchaine, High and low flowrate sampling of airborne influenza in hospital rooms during three outbreaks, J. Aerosol Sci. 158 (2021), 105824, https://doi.org/10.1016/j.jaerosci.2021.105824.
[36] T. Han, H. Park, Y. Jeong, J. Lee, E. Shon, M.-S. Park, M. Sung, COVID-19 cluster linked to aerosol transmission of SARS-CoV-2 via floor drains, J. Infect. Dis. (2022), https://doi.org/10.1093/infdis/jiab598 jiab598.
[37] Coronavirus: How infected air can flow from one apartment to another, Elpais. (n. d.). https://elpais.com/especiales/coronavirus-covid-19/how-infected-air-can-flow-from-one-apartment-to-another/ (accessed April 13, 2022).
[38] S.J. Emmerich, D. Heinzerling, J. il Choi, A.K. Persily, Multizone modeling of strategies to reduce the spread of airborne infectious agents in healthcare facilities, Build. Environ. 60 (2013) 105–115, https://doi.org/10.1016/j.buildenv.2012.11.013.
[39] L.F. Pease, N. Wang, T.I. Salsbury, R.M. Underhill, J.E. Flaherty, A. Vlachokostas, G. Kulkarni, D.P. James, Investigation of potential aerosol transmission and infectivity of SARS-CoV-2 through central ventilation systems, Build. Environ. 197 (2021), 107633, https://doi.org/10.1016/j.buildenv.2021.107633.
[40] P. Shrestha, J.W. DeGraw, M. Zhang, X. Liu, Multizonal modeling of SARS-CoV-2 aerosol dispersion in a virtual office building, Build. Environ. 206 (2021), 108347, https://doi.org/10.1016/j.buildenv.2021.108347.
[41] J. Guo, J. Liu, D. Tu, J. Zhang, J. Xu, P. Xue, Multizone modeling of pressure difference control analyses for an infectious disease hospital, Build. Environ. 206 (2021), 108341, https://doi.org/10.1016/j.buildenv.2021.108341.

[42] C.A. Faulkner, J.E. Castellini, W. Zuo, D.M. Lorenzetti, M.D. Sohn, Investigation of HVAC operation strategies for office buildings during COVID-19 pandemic, Build. Environ. (2021), 108519, https://doi.org/10.1016/j.buildenv.2021.108519.
[43] M. López-García, M.-F. King, C.J. Noakes, A multicompartment SIS stochastic model with zonal ventilation for the spread of nosocomial infections: detection, outbreak management, and infection control, Risk Anal. 39 (2019) 1825–1842, https://doi.org/10.1111/risa.13300.
[44] W.S. Dols, B.J. Polidoro, CONTAMW User Guide and Program Documentation, National Institute of Standards and Technology, Gaithersburg, MD, USA, MD, 2016.
[45] LNBL, EnergyPlus Engineering Reference, Washington, 2012.
[46] G.N. Walton, AIRNET - a Computer Program for Building Airflow Network Modeling, National Institute of Standards and Technology, Gaithersburg, MD, 1989.
[47] H.E. Feustel, COMIS - an international multizone air-flow and contaminant transport model, Energy Build. 30 (1999) 3–18.
[48] NIST, Fate and Transport of Indoor Microbiological Aerosols (FaTIMA), NIST, 2021.
[49] W.S. Dols, B.J. Polidoro, D. Poppendieck, S.J. Emmerich, NIST Technical Note 2095 A Tool to Model the Fate and Transport of Indoor Microbiological Aerosols, FaTIMA, 2020, https://doi.org/10.6028/NIST.TN.2095.
[50] W.S. Dols, B.J. Polidoro, D. Poppendieck, S.J. Emmerich, A Tool to Model the Fate and Transport of Indoor Microbiological Aerosols, FaTIMA, Gaithersburg, MD, 2020, https://doi.org/10.6028/NIST.TN.2095.
[51] L.L. Wang, W.S. Dols, Q. Chen, Using CFD capabilities of CONTAM 3.0 for simulating airflow and contaminant transport in and around buildings, HVAC\&R Res. 16 (2010) 749–763, https://doi.org/10.1080/10789669.2010.10390932.
[52] L. Wang, Q. Chen, Validation of a coupled multizone-CFD program for building airflow and contaminant transport simulations, HVAC\&R Res. 13 (2007) 267–281, https://doi.org/10.1080/10789669.2007.10390954.
[53] W. Wells, Airborne contagion and air hygiene: an ecological study of droplet infections, J. Am. Med. Assoc. 159 (1955) 90, https://doi.org/10.1001/jama.1955.02960180092033.
[54] N. van Doremalen, T. Bushmaker, D.H. Morris, M.G. Holbrook, A. Gamble, B. N. Williamson, A. Tamin, J.L. Harcourt, N.J. Thornburg, S.I. Gerber, J.O. Lloyd-Smith, E. de Wit, V.J. Munster, Aerosol and surface stability of SARS-CoV-2 as compared with SARS-CoV-1, N. Engl. J. Med. 382 (2020) 1564–1567, https://doi.org/10.1056/NEJMc2004973.
[55] G.R. Johnson, L. Morawska, Z.D. Ristovski, M. Hargreaves, K. Mengersen, C.Y. H. Chao, M.P. Wan, Y. Li, X. Xie, D. Katoshevski, S. Corbett, Modality of human expired aerosol size distributions, J. Aerosol Sci. 42 (2011) 839–851, https://doi.org/10.1016/j.jaerosci.2011.07.009.
[56] NAFA Technical Committee, Methods of Testing General Ventilation Air-Cleaning Devices for Removal Efficiency by Particle Size, 2018.
[57] S. Miller-Leiden, C. Lohascio, W.W. Nazaroff, J.M. Macher, Effectiveness of in-room Air filtration and dilution ventilation for tuberculosis infection control, J. Air \& Waste Manag. Assoc. 46 (1996) 869–882, https://doi.org/10.1080/10473289.1996.10467523.
[58] US DOE, Commercial Prototype Building Models | Building Energy Codes Program, U.S. Dep. Energy, 2013.
[59] ASHRAE, ASHRAE 62.1-2013 Ventilation for Acceptable Indoor Air Quality, ASHRAE, 2013.
[60] S.N. Rudnick, D.K. Milton, Risk of indoor airborne infection transmission estimated from carbon dioxide concentration, Indoor Air 13 (2003) 237–245, https://doi.org/10.1034/j.1600-0668.2003.00189.x.
[61] T. Moreno, R.M. Pintó, A. Bosch, N. Moreno, A. Alastuey, M.C. Minguillón, E. Anfruns-Estrada, S. Guix, C. Fuentes, G. Buonanno, L. Stabile, L. Morawska, X. Querol, Tracing surface and airborne SARS-CoV-2 RNA inside public buses and subway trains, Environ. Int. 147 (2021), 106326, https://doi.org/10.1016/j.envint.2020.106326.
[62] L. Ng, A. Musser, A. Persily, S. Emmerich, Airflow and indoor air quality models of DOE prototype commercial buildings. https://doi.org/10.6028/NIST.TN.2072, 2019.
[63] ASHRAE, ANSI/ASHRAE/IES Standard 90.1-2013: Energy Standard for Buildings except Low-Rise Residential Buildings, American Society of Heating, Refrigerating and Air-Conditioning Engineers, Atlanta), 2013.
[64] B. Polidoro, L.C. Ng, W.S. Dols, S.J. Emmerich, NIST Technical Note 1873: CONTAM to EnergyPlus Infiltration Features of the CONTAM Results Export Tool, Gaithersburg, 2015.
[65] L. Ng, A. Musser, A.K. Persily, S. Emmerich, Airflow and Indoor Air Quality Models of DOE Reference Commercial Buildings, National Institute of Standards and Technology, Gaithersburg, MD, 2012.
[66] U.S.EPA, Exposure Factors Handbook 2011 Edition (Final Report), Washington, 2011.
[67] E. Diapouli, A. Chaloulakou, P. Koutrakis, Estimating the concentration of indoor particles of outdoor origin: a review, J. Air \& Waste Manag. Assoc. 63 (2013) 1113–1129, https://doi.org/10.1080/10962247.2013.791649.
[68] T.L. Thatcher, A.C.K. Lai, R. Moreno-Jackson, R.G. Sextro, W.W. Nazaroff, Effects of room furnishings and air speed on particle deposition rates indoors, Atmos. Environ. 36 (2002) 1811–1819, https://doi.org/10.1016/S1352-2310(02)00157-7.
[69] N. Van Doremalen, T. Bushmaker, D.H. Morris, M.G. Holbrook, A. Gamble, B. N. Williamson, A. Tamin, J.L. Harcourt, N.J. Thornburg, S.I. Gerber, J.O. Lloyd-Smith, E. De Wit, V.J. Munster, Aerosol and surface stability of SARS-CoV-2 as compared with SARS-CoV-1, N. Engl. J. Med. 382 (2020) 1564–1567, https://doi.org/10.1056/NEJMc2004973.
[70] S.L. Miller, J.M. MacHer, Evaluation of a methodology for quantifying the effect of room Air ultraviolet germicidal irradiation on airborne bacteria, Aerosol Sci. Technol. 33 (2000) 274–295, https://doi.org/10.1080/027868200416259.
[71] E. Kujundzic, M. Hernandez, S.L. Miller, Ultraviolet germicidal irradiation inactivation of airborne fungal spores and bacteria in upper-room air and HVAC induct configurations, J. Environ. Eng. Sci. 6 (2007) 1–9, https://doi.org/10.1139/s06-039.
[72] J. Pan, C. Harb, W. Leng, L.C. Marr, Inward and outward effectiveness of cloth masks, a surgical mask, and a face shield, Aerosol Sci. Technol. 55 (2021) 718–733, https://doi.org/10.1080/02786826.2021.1890687.
[73] H. Qian, T. Miao, L. Liu, X. Zheng, D. Luo, Y. Li, Indoor transmission of SARS-CoV-2, Indoor Air 31 (2021) 639–645, https://doi.org/10.1111/ina.12766.
[74] D. Weissberg, J. Böni, S.K. Rampini, V. Kufner, M. Zaheri, P.W. Schreiber, I. A. Abela, M. Huber, H. Sax, A. Wolfensberger, Does respiratory co-infection facilitate dispersal of SARS-CoV-2? investigation of a super-spreading event in an open-space office, Antimicrob. Resist. Infect. Control. 9 (2020) 191, https://doi.org/10.1186/s13756-020-00861-z.
[75] B. Atkinson, K. van Veldhoven, I. Nicholls, M. Coldwell, A. Clarke, G. Frost, C. J. Atchison, A.I. Raja, A.M. Bennett, D. Morgan, N. Pearce, T. Fletcher, E. B. Brickley, Y. Chen, An Outbreak of SARS-CoV-2 in a Public-Facing Office in England, MedRxiv, 2022, https://doi.org/10.1101/2022.01.31.22269194, 2021.
[76] B.L. Augenbraun, Z.D. Lasner, D. Mitra, S. Prabhu, S. Raval, H. Sawaoka, J. M. Doyle, Assessment and mitigation of aerosol airborne SARS-CoV-2 transmission in laboratory and office environments, J. Occup. Environ. Hyg. 17 (2020) 447–456, https://doi.org/10.1080/15459624.2020.1805117.
[77] S.J. Emmerich, Validation of multizone IAQ modeling of residential-scale buildings: a review, Trans. Soc. Heat. Refrig. Air Cond. Eng. 107 (2001) 619–628.
[78] S.J. Emmerich, S.J. Nabinger, Measurement and simulation of the IAQ impact of particle air cleaners in a single-zone building, Hvac&R Res. 7 (2001) 223–244.
[79] S.L. Miller, W.W. Nazaroff, J.L. Jimenez, A. Boerstra, G. Buonanno, S.J. Dancer, J. Kurnitski, L.C. Marr, L. Morawska, C. Noakes, Transmission of SARS-CoV-2 by inhalation of respiratory aerosol in the Skagit Valley Chorale superspreading event, Indoor Air 31 (2021) 314–323, https://doi.org/10.1111/ina.12751.
[80] REHVA, COVID-19 Ventilation Calculator, 2020.